Structural and Functional Evaluation of Clinically-Relevant Inhibitors of Steroidogenic Cytochrome P450 17A1 (CYP17A1)

Elyse M. Petrunak, Steven A. Rogers, Jeffrey Aubé, and Emily E. Scott

Department of Medicinal Chemistry, University of Kansas, Lawrence, Kansas, 66045

1

DMD # 75317

Running Title: Structure and Function of Cytochrome P450 17A1 Inhibitors

Corresponding Author: Emily E. Scott, Department of Medicinal Chemistry, University of Michigan, 428 Church St., Ann Arbor, MI 48109, 734-764-3530, scottee@umich.edu

Paper Statistics:

Text Pages: 21.1

Tables: 3

Figures: 8

References: 42

Words in Abstract: 239

Words in Introduction: 726

Words in Discussion: 1500

Nonstandard abbreviations: CYP17A1, human cytochrome P450 17A1; K_d, dissociation constant

ABSTRACT

Human steroidogenic cytochrome P450 17A1 (CYP17A1) is a bifunctional enzyme that performs both hydroxylation and lyase reactions, with the latter required to generate androgens that fuel prostate cancer proliferation. The steroid abiraterone, the active form of the only FDA-approved CYP17A1 inhibitor, binds the catalytic heme iron, nonselectively impeding both reactions and ultimately causing undesirable corticosteroid imbalance. Some non-steroidal inhibitors reportedly inhibit the lyase reaction more than the preceding hydroxylase reaction, which would be clinically advantageous, but the mechanism is not understood. Thus, the non-steroidal inhibitors seviteronel and orteronel and the steroidal inhibitors abiraterone and galeterone were compared with respect to their binding modes and hydroxylase vs. lyase inhibition. Binding studies and X-ray structures of CYP17A1 with non-steroidal inhibitors reveal coordination to the heme iron like the steroidal inhibitors. (*S*)-Seviteronel binds similarly to both observed CYP17A1 conformations. However, (*S*)-orteronel and (*R*)-orteronel bind to distinct CYP17A1 conformations that differ in a region implicated in ligand entry/exit and the presence of a peripheral ligand. To reconcile these binding modes with enzyme function, side-by-side enzymatic analysis was undertaken and revealed that neither the non-steroidal seviteronel or (*S*)-orteronel inhibitors demonstrated significant lyase selectivity, but the less potent (*R*)-orteronel was 8- to 11-fold selective for lyase inhibition. While active site iron coordination is consistent with competitive inhibition, conformational selection for binding of some inhibitors and the differential presence of a peripheral ligand molecule suggest the possibility of CYP17A1 functional modulation by features outside the active site.

3

INTRODUCTION

Among American men, prostate cancer is the most frequently diagnosed cancer and second-leading cause of cancer-related deaths (Edwards et al., 2014). More than 80% of prostate cancers rely on androgens for tumor growth (Geller, 1993; Yin and Hu, 2014) and blocking their production can hinder disease progression. Traditional androgen deprivation therapy targets the gonadotropin-releasing hormone receptor to ultimately inhibit testicular androgen production. However, adrenal androgens are still produced, often requiring coadministration of androgen receptor antagonists (Yin and Hu, 2014). Despite these measures, most patients relapse within 24 months with castration-resistant prostate cancer (Gomez et al., 2015) fueled by androgens from the adrenal gland or tumor (Montgomery et al., 2008). Castration-resistant prostate cancer can be treated by inhibition of cytochrome P450 17A1 (CYP17A1), a required steroidogenic enzyme in all such tissues.

CYP17A1 converts 21-carbon steroids to 19-carbon androgens in two chemical transformations (Arlt et al., 2002). First, 21-carbon pregnenolone or progesterone is hydroxylated (Figure 1A). The 17α-hydroxypregnenolone product can undergo a second, 17,20-lyase reaction in the same active site to yield 19-carbon dehydroepiandrosterone, the androgen precursor for all sex steroids (Figure 1A). 17α-Hydroxylated steroids are also intermediates in glucocorticoid biosynthesis (Gilep et al., 2011) (Figure 1A). Thus, mutations or clinical inhibition impacting both CYP17A1 reactions block androgen and glucocorticoid production. Glucocorticoid deficiency drives adrenocorticotropin hormone secretion, resulting in mineralocorticoid overproduction manifested clinically as hypertension, hypokalemia, and peripheral edema (Auchus, 2001). This occurs in prostate cancer patients treated with the otherwise effective, first-in-class CYP17A1 inhibitor abiraterone acetate (Attard et al., 2008).

4

Abiraterone acetate is an ester prodrug rapidly hydrolyzed *in vivo* to the active alcohol form. Abiraterone (Table 1) is essentially the substrate pregnenolone with addition of a pyridine ring (Potter et al., 1995). The pyridine coordinates the heme necessary for both CYP17A1-mediated reactions (Figure 1B) (DeVore and Scott, 2012). Abiraterone effectively reduces serum androgens (O'Donnell et al., 2004; Ryan et al., 2010) and increases overall survival (Fizazi et al., 2012) in prostate cancer patients, but the associated hypertension and peripheral edema reaction require prednisone coadministration (Attard et al., 2012).

Several new CYP17A1 inhibitors have entered clinical trials (Table 1), including the steroidal inhibitor galeterone (VN/124-1 or TOK-001) (Handratta et al., 2005) and non-steroidal, naphthalene-based inhibitors (*S*)-orteronel (TAK-700) (Yamaoka et al., 2012) and (*S*)-seviteronel (VT-464) (Rafferty et al., 2014). These non-steroidal inhibitors reportedly selectively inhibit the lyase reaction while sparing the 17-hydroxylase activity necessary for glucocorticoid biosynthesis. The reported selectivity is modest (5- (Yamaoka et al., 2012) and 10-fold (Rafferty et al., 2014) for (*S*)-orteronel and (*S*)-seviteronel, respectively), but improved over that of abiraterone (0.1- to 1.4-fold (Potter et al., 1995; Yamaoka et al., 2012; Rafferty et al., 2014)). No selectivity information is available for galeterone. Reports of lyase-selective inhibition are intriguing as all of these inhibitors contain nitrogen-containing heterocycles, which often coordinate the heme iron and should indiscriminately inhibit both CYP17A1 reactions. However, there are no structures of CYP17A1 with non-steroidal inhibitors to inform on their binding modes.

Additionally, functional comparisons between these inhibitors are frequently frustrated by differences between experimental conditions and systems used to evaluate them. Both 17,20-lyase and hydroxylase inhibition studies use a wide range of substrate concentrations, which can

influence the apparent IC_{50} depending on inhibition mode. Additionally, the 17α-hydroxylase reaction has two different physiological substrates, progesterone and pregnenolone, which demonstrate distinct CYP17A1 affinities and are hydroxylated at different rates (Petrunak et al., 2014), yet inhibition studies are typically conducted with a single hydroxylase substrate, the identity of which varies between reports. To add complexity, CYP17A1 requires NADPH-cytochrome P450 reductase for both reactions, whereas cytochrome b_5 substantially augments only the 17,20-lyase reaction (Katagiri et al., 1995; Auchus et al., 1998). The systems in which these partner proteins are produced and incorporated with CYP17A1 vary among inhibition studies. Differences in expression system (yeast vs. *Escherichia coli*), relative amounts of enzyme system components, and preparation of enzyme system (microsomal vs. purified proteins vs. whole cell) can all undermine comparisons of IC_{50} values between studies.

The present study employs spectral binding studies and X-ray structures with the non-steroidal inhibitors to reveal Fe coordination similar to steroidal inhibitors, but with conformational selection and a peripheral ligand binding pocket in some cases. To probe the relationships between these binding modes and enzyme inhibition, both steroidal and non-steroidal inhibitors were then rigorously evaluated and compared for their ability to selectively inhibit the CYP17A1 17,20-lyase reaction vs. both 17α-hydroxylase reactions.

MATERIALS AND METHODS

Materials

Abiraterone and orteronel were purchased from Selleckchem (Houston, TX). Abiraterone is used in these studies instead of the prodrug abiraterone acetate (Zytiga®) because

abiraterone is the active form *in vivo*. Galeterone was purchased from Chemexpress (Shanghai, China).

Racemic seviteronel was synthesized as reported (Rafferty et al., 2014). The racemic mixture was separated into enantiomers using a preparative HPLC with an IA chiral column (Chiralpak particle size 5 μm, dimensions 20mm x 250mm), a guard column (particle size 5 μm, dimensions 21mm x 50mm), and an *n*-hexanes/isopropanol mobile phase (flow rate: 15 mL/min). The retention times for (*S*)-seviteronel and (*R*)-seviteronel were 26.8 min and 28.2 min, respectively (measured on an IA chiral analytical column). (*S*)-Seviteronel was isolated as 56 mg of a white powder with a specific rotation of $[\alpha]_D^{RT}$ –63 (*c* 0.5, methanol) and enantiomeric ratio (er) of 99:1 as measured by analytical HPLC (Agilent 1100 series) with an analytical chiral column (Chiralcel OD-H, particle size 5 μm, dimensions 4.6 mm x 150mm) while using a mobile phase of *n*-hexanes:isopropanol. Similarly, (*R*)-seviteronel was isolated as 49 mg of a white powder: $[\alpha]_D^{RT}$ 59 (*c* 0.5, MeOH), and er = 99.6:0.4.

The commercial orteronel was also separated into its enantiomers using the same preparative HPLC system described above, except employing an OD-H SFC column. The retention times for (*S*)-orteronel and (*R*)-orteronel were 24.0 min and 25.7 min, respectively (measured on an OD-H/SFC chiral analytical column). All binding and enzymatic assays were accomplished with the individual enantiomers of each compound.

All compounds were >95% pure as evaluated by HPLC by either the respective suppliers and/or in house evaluation.

CYP17A1 with a modified 19-residue truncation of the N-terminus and addition of a C-terminal 4 x histidine tag was expressed in *Escherichia coli* JM109 cells and purified as reported previously (Petrunak et al., 2014). Human NADPH cytochrome P450 reductase bearing an N-

terminal truncation and a mutation to decrease proteolysis (K59Q), and full-length rat

cytochrome b_5 were expressed and purified according to previously described protocols (Sandee

and Miller, 2011).

Spectral ligand binding assays

Inhibitor binding to 100 nM CYP17A1 was monitored by measuring changes in

absorbance associated with the heme cofactor as described previously (Petrunak et al., 2014).

Notably, this low protein concentration was dictated by the very tight binding of most of the

inhibitors (Copeland, 2013) and partially compensated for by using cuvettes with a 5 cm path

length to improve signal/noise. The change in absorbance after each addition of inhibitor (ΔA)

was plotted vs. the inhibitor concentration (S). Graphpad Prism was used to determine the K_d

and ΔA_{max} with non-linear least-squares regression fitting to the Morrison equation, also known

as the tight-binding equation, where E is total protein concentration and S is total ligand

concentration:

$$\Delta A = \Delta A_{max} \frac{(E + S + K_d) - \sqrt{(E + S + K_d)^2 - 4ES}}{2E}$$

Crystallization and Structure Determination

CYP17A1 was co-crystallized with orteronel or (*S*)-seviteronel via hanging drop vapor

diffusion. Based on our experience with other CYP17A1 ligands with limited solubility, purified

CYP17A1 was serially exchanged into ligand-containing buffer. Ligand-free CYP17A1 in 50

mM Tris HCl, pH 7.4, 20% glycerol, 500 mM NaCl, and 100 mM glycine was diluted 5-fold in

the same buffer containing either 100 μM orteronel (a mixture of enantiomers from

Selleckchem) or 500 μM (*S*)-seviteronel and concentrated together. This dilution and

concentration in ligand-containing buffer was repeated multiple times to saturate CYP17A1,

followed by concentration to 29-30 mg/mL. The solubility of (*S*)-seviteronel permitted addition

8

of additional ligand to a final concentration of 1 mM. Emulgen-913 (Desert Biologicals) was then added to a concentration of 0.5% (v/v). This protein/ligand/detergent stock solution (1 μl) was mixed with 1 μl precipitant to form 2 μL drops. The precipitant solution used to crystallize CYP17A1 with orteronel was 175 mM Tris HCl, pH 8.0, 30% (w/v) PEG-3350, 200 mM Li_2SO_4, and 12% glycerol. The precipitant solution used to crystallize CYP17A1 with (*S*)-seviteronel was 100 mM sodium cacodylate trihydrate, pH 6.5, 200 mM ammonium sulfate, and 30% (w/v) PEG-8000. The 2 μL drop used to generate (*S*)-seviteronel crystals was seeded with microcrystals generated in a 1 μL drop via sitting drop vapor diffusion in a 1:1 ratio with precipitant. The 2 μL drops were equilibrated against 750 μL of the respective precipitant at 20 °C, whereas the 1 μL drops were equilibrated against 100 μL precipitant at the same temperature. Crystals were cryoprotected using a 7:3 mixture of mother liquor to 80% glycerol and were flash cooled in liquid nitrogen.

Data were collected on beamline 12-2 or 7-1 at the Stanford Synchrotron Radiation Lightsource and processed using XDS (Kabsch, 2010). Parameters for data collection and refinement statistics are described in Table 2. Structures were solved by molecular replacement in Phaser (McCoy et al., 2007) using a previous structure of CYP17A1 with heme cofactor (PDB ID: 3SWZ (DeVore and Scott, 2012)) as a search model and data to the corresponding resolution cutoff (2.2 Å for CYP17A1 with orteronel and 3.15 Å for CYP17A1 with (*S*)-seviteronel). Model-building and iterative refinement were performed using COOT (Emsley et al., 2010) and PHENIX (Adams et al., 2010), respectively. Ligand models were generated using eLBOW in PHENIX (Adams et al., 2010). Simulated-annealing $2F_o$-F_c and F_o-F_c composite omit maps were calculated in PHENIX (Adams et al., 2010). Figures were generated using PyMOL (Schrodinger, 2010).

9

Enzyme inhibition assays

Inhibition of progesterone hydroxylation by both steroidal and non-steroidal compounds (0-30 μM) was evaluated using a 1:4 ratio of CYP17A1 (50 pmol) and human NADPH-cytochrome P450 reductase (200 pmol) at a substrate concentration of 10 μM, which is the previously determined K_m for this reaction (Petrunak et al., 2014). This assay was carried out as previously described (DeVore and Scott, 2012; Petrunak et al., 2014), using HPLC/UV-vis to quantify 17α-hydroxyprogesterone. Inhibition of pregnenolone hydroxylation by steroidal and non-steroidal compounds (0-60 μM) was evaluated using the same 1:4 ratio of CYP17A1 (50 pmol) and human reductase (200 pmol) at a substrate concentration of 1 μM, which is the previously determined K_m for this reaction (Petrunak et al., 2014). 17α-Hydroxypregnenolone 17,20-lyase inhibition by steroidal and non-steroidal compounds (0-10 μM) was evaluated using the same 1:4 ratio of CYP17A1 (50 pmol) to human reductase (200 pmol), with the addition of rat cytochrome b_5 (200 pmol) and using a substrate concentration of 1.2 μM, which is the previously determined K_m for this reaction (Petrunak et al., 2014). GC/MS was used to quantify the silylated products 17α-hydroxypregnenolone (for pregnenolone hydroxylase inhibition) and dehydroepiandrosterone (for 17α-hydroxypregnenolone 17,20-lyase inhibition) (Petrunak et al., 2014). All three assays were initiated by addition of NADPH, carried out for 20 min at 37 °C in a total volume of 500 μl (100 nM CYP17A1) as previously reported (Petrunak et al., 2014). In no case was the amount of substrate converted to product greater than 6%. Data were fit to the equation for log [inhibitor] vs. normalized response (Variable Slope) in Graphpad Prism. IC$_{50}$ values are the average of two independent experiments spanning the entire inhibitor concentration range and are reported ± standard error. Within each experiment, each individual

10

inhibitor concentration was evaluated in duplicate or triplicate and the variation in these technical replicates are typified by the error bars in Figure 8.

RESULTS

Binding of Non-steroidal Inhibitors to CYP17A1

To monitor non-steroidal inhibitor binding in the CYP17A1 active site, the purified enzyme was titrated with (*S*)-orteronel and (*S*)-seviteronel and changes in UV-vis spectra were monitored from 500 to 300 nm. Since both compounds include a single stereogenic center, the corresponding (*R*)-orteronel and (*R*)-seviteronel enantiomers were also evaluated for binding affinity to CYP17A1. Binding of all four non-steroidal compounds resulted in an increase in absorbance at 424 nm and a decrease in absorbance at 393-410 nm (Figure 2). This observed spectral shift is consistent with a change in heme electronic configuration upon replacement of the iron-water complex with a complex in which the iron is coordinated to a ligand heteroatom (Jefcoate, 1978). This observation suggests that the nitrogen heterocycles of the non-steroidal inhibitors participate in heme coordination similar to those of the steroidal inhibitors abiraterone (Figure 1B) and galeterone (DeVore and Scott, 2012).

For each titration, the change in absorbance as a function of ligand concentration was fit to the Morrison equation, also known as the tight-binding equation, to determine the dissociation constant of the CYP17A1-inhibitor complex. (*S*)-Orteronel, (*R*)-orteronel, and (*S*)-seviteronel demonstrated very high affinity, with estimated K_d values of 40 ± 7, 56 ± 8, and 31 ± 7 nM, respectively. Such high affinity is clear from the titration data (Figure 3A), in which the change in absorbance is essentially linear with respect to ligand concentration until no free CYP17A1 remains, beyond which no further absorbance change occurs. The result is a poor fit even to the

11

Morrison equation. Binding of CYP17A1 to steroidal inhibitors abiraterone and galeterone previously resulted in tight binding and similar deviations (DeVore and Scott, 2012). Therefore, the estimated K_d values probably represent the upper limit for these K_d values and these ligands likely bind much more tightly than estimated. In contrast, (*R*)-seviteronel bound to CYP17A1 with lower affinity, demonstrating a more typical hyperbolic curve and a K_d of 290 ± 10 nM (Figure 3B). Although a rank order affinity cannot be established for most of the non-steroidal inhibitors, (*R*)-seviteronel is clearly a lower affinity ligand for CYP17A1 compared to (*S*)-seviteronel and both enantiomers of orteronel.

Crystal Structure of CYP17A1 with Orteronel

To probe the basis for the reported 5-fold selective inhibition of the 17,20-lyase vs. hydroxylase reactions, purified CYP17A1 was co-crystallized with commercial material purchased as (*S*)-orteronel (Selleckchem). The resulting structure of CYP17A1 was determined at 2.2 Å resolution in the space group $P2_12_12_1$. This is the same space group as previous CYP17A1 structures with both steroidal inhibitors and steroid substrates (DeVore and Scott, 2012; Petrunak et al., 2014). The overall protein structure was consistent with the aforementioned structures, with four molecules composing the asymmetric unit. Also in agreement with previous structures of CYP17A1, there is high structural similarity between molecules A and B (rmsd over all Cα = 0.28 Å), and between molecules C and D (rmsd over all Cα = 0.42 Å), but more substantial differences are observed when comparing molecules A/B against C/D (average rmsd over all Cα = 1.20 ± 0.02 Å). These two CYP17A1 conformation primarily differ at the N-terminus and the region between the F and G helices, as described for previous structures of CYP17A1 (Petrunak et al., 2014).

DMD # 75317

Clear density was observed for orteronel in the active sites of all four CYP17A1 molecules in the crystal, and unambiguously indicates that the ligand is coordinated to the heme iron (Figure 4), consistent with the spectral shifts observed upon ligand binding. However, the remainder of the ligand density observed in the active sites of molecules A and B was significantly different compared to that observed in molecules C and D. Ligand density in molecules C and D was clearly (*S*)-orteronel (Figure 4A), however, this ligand was clearly not a match for the density observed in the active sites of molecules A and B. The inconsistent ligand density observed in the two different conformations of CYP17A1 led to in-house characterization of the commercially-purchased (*S*)-orteronel, which was found to actually contain both enantiomers of orteronel along with small amounts of an unidentified impurity. (*R*)-Orteronel provides a good fit for the ligand density in molecules A and B (Figure 4B) and is consistent with the $2F_o$-F_c map, although the F_o-F_c difference maps are not completely satisfied by modeling this ligand in a single orientation, which may indicate a small amount of disorder.

(*R*)-Orteronel bound in the CYP17A1 active is oriented similar to steroidal substrates and inhibitors, at a 60° angle from the plane of the heme, with one face of the naphthalene ring positioned flat against the I helix and the oxygen of the amide substituent directed toward a residue on the F helix, asparagine 202 (Figure 5B). This residue has been shown to hydrogen bond with the C3 substituent of steroidal inhibitors and substrates, and appears to participate in a hydrogen bond (distances of 3.4 and 3.0 Å for molecules A and B, respectively) with (*R*)-orteronel as well.

The orientation of (*S*)-orteronel in the active site of molecules C/D shares some characteristics with (*R*)-orteronel as well as steroidal inhibitors and substrates. This ligand also forms an approximate 60° angle from the plane of the heme, with one face of the naphthalene

13

core positioned flat against the I helix. However, in contrast to (*R*)-orteronel and steroidal inhibitors, (*S*)-orteronel is oriented toward the G helix (Figure 5A) instead of the F helix. The amide substituent hydrogen bonds with arginine 239 (R239; H-bonding distance of 2.7 and 3.0 Å for molecules C and D, respectively) and aspartic acid 298 (D298; H-bonding distance of 2.7 and 2.8 Å for molecules C and D respectively) on the I helix. Even though the F and G helices and other features of the active sites are essentially the same, these differential interactions are correlated with the two distinct conformations of the intervening F/G region.

Crystal Structure of CYP17A1 with (*S*)-seviteronel

Of the two non-steroidal CYP17A1 inhibitors to enter clinical trials, (*S*)-Seviteronel was reportedly the most selective, with 10-fold more potent 17,20-lyase inhibition (Rafferty et al., 2014). The crystal structure of CYP17A1 bound to (*S*)-seviteronel was determined at 3.1 Å in the space group $P2_12_12_1$. The asymmetric unit comprised four copies of CYP17A1, which were similar to previous structures of CYP17A1 with substrates and inhibitors, including that of CYP17A1 with orteronel. As described above for the CYP17A1/orteronel structure, molecules A and B demonstrated very similar overall conformation, as did molecules C and D. Less structural similarity was observed between molecules A/B and C/D because of the same conformational differences at the N-terminus and F/G loop observed in the previous CYP17A1 structures.

Density corresponding to (*S*)-seviteronel is present in all four copies of CYP17A1 (Figure 6A), and was consistent between all copies. The density clearly indicates that the ligand is coordinated to the heme iron, consistent with the spectral shift observed upon ligand binding. As with orteronel, the naphthalene ring is positioned flat against the I helix. However, unlike the structures with all other CYP17A1 inhibitors, (*S*)-seviteronel does not appear to form hydrogen

14

bonds with any residues in the F or G helices (Figure 6B). Instead, the hydroxyl group participates in a hydrogen bond with the backbone carbonyl of V482 (average distance over four molecules = 2.9 ± 0.1 Å), while one of the nitrogens of the triazole coordinated to the heme iron is positioned within hydrogen bonding distance of the T306 side chain (average distance over four molecules = 3.1 ± 0.2 Å). The difluoromethoxy substituents of the inhibitor can be modeled in varied orientations within the CYP17A1 active site depending on the molecule, but generally position the fluorine atoms within 3.0 Å of active site residues including asparagine 202 and arginine 239. It is possible that the difluoromethoxy substituents participate in weak dipolar or multipolar interactions with the side chains of these residues.

Peripheral ligand binding site

In all CYP17A1 complexes, both those determined here with nonsteroidal inhibitors and those reported previously with steroids, two distinct, well-defined conformations are observed for the residues between the F and G helices, though the positions of the flanking helices are largely conserved (Figure 7). The membrane-embedded region between these helices has been implicated in access of hydrophobic ligands to the otherwise buried active site. In the orteronel structure reported herein, strong, continuous density consistent with binding of a peripheral ligand was observed between the F/G loop and N-terminal residues (Fo-Fc map at 3σ in Figure 7), but in only one of the two CYP17A1 conformations (teal in Figure 7). This is the same CYP17A1 conformation (molecules C/D) that binds (*S*)-orteronel. The CYP17A1 conformation to which (*R*)-orteronel binds in the active site (molecules A/B) has a conformation of the F/G loop that does not permit peripheral ligand binding (magenta in Figure 7). In the structure of CYP17A1 with (*S*)-seviteronel, electron density is observed in the peripheral binding site only for the CYP17A1 C/D conformation that also binds (*S*)-orteronel, but this electron density is

weaker in the (*S*)-seviteronel structure. This may be due to lower ligand affinity, more disorder, or, more likely, the lower resolution of the (*S*)-seviteronel structure. Most of the residues surrounding this peripheral ligand are hydrophobic, suggesting a site that might have relatively low specificity. In the higher resolution structure with orteronel, this peripheral density was experimentally modeled as either orteronel enantiomer, as a combination of enantiomers, and at partial occupancies. Based on decreases in R and R_{free} and comparison of the electron density and the ligand contours, (*R*)-orteronel was the best match, but not good enough to unambiguously model (*R*)-orteronel. A partially occupied, low-affinity peripheral steroid binding site has been identified in the F/G region of structures of the steroidogenic CYP21A2 (Zhao et al., 2012; Pallan et al., 2015b).

Inhibition of Targeted 17,20-Lyase Reaction

To probe and compare relationships between the Fe-N binding mode observed in crystals and in solution with the functional consequences, steroidal inhibitors (abiraterone and galeterone), non-steroidal inhibitors from clinical trials ((*S*)-orteronel and (*S*)-seviteronel), and their corresponding enantiomers ((*R*)-orteronel and (*R*)-seviteronel) were initially evaluated for inhibition of the 17,20-lyase reaction, which is desirable for treatment of prostate cancer. IC_{50} determination was conducted using the physiologically-relevant substrate 17α-hydroxypregnenolone at a concentration corresponding to the previously determined K_m of this reaction (1.2 μM (Petrunak et al., 2014)) and in the presence of cytochrome b_5, which is the physiologically-relevant stimulator of the lyase reaction. The resulting IC_{50} values are shown in Table 3.

The FDA-approved, first-in-class CYP17A1 inhibitor abiraterone demonstrated the highest potency for 17,20-lyase inhibition. The other steroidal inhibitor, galeterone, was ca. 3-

16

fold less potent than abiraterone, but still showed higher potency than any of the non-steroidal inhibitors. Of the non-steroidal inhibitors, (*S*)-orteronel exhibited only 6-fold lower potency than abiraterone, while (*R*)-orteronel exhibited nearly 13-fold lower potency compared to abiraterone. Finally, (*S*)-seviteronel and (*R*)-seviteronel were 12-fold and ~140-fold less potent than abiraterone, respectively.

Inhibition of Off-Target Progesterone and Pregnenolone Hydroxylation Reactions

Each inhibitor was subsequently also evaluated for inhibition of progesterone and pregnenolone hydroxylation reactions. Such inhibition is undesirable for treating prostate cancer. Consistent with the 17,20-lyase inhibition assay, these reactions were also performed using purified human CYP17A1 and NADPH cytochrome P450 reductase and substrate concentrations equal to the previously determined K_m values of these reactions (10 μM and 1 μM for progesterone and pregnenolone hydroxylation, respectively) using the same experimental parameters. Since the hydroxylase reactions do not appear to require cytochrome b_5 physiologically, this protein was not included in the *in vitro* enzyme system to prevent subsequent conversion of the hydroxylase product to the corresponding 19-carbon androgen via the 17,20-lyase reaction. IC$_{50}$ values are shown in Table 3.

The rank order potencies for inhibition of the off-target hydroxylation reactions were similar to that of 17,20-lyase inhibition. Abiraterone displayed the greatest potency, followed by the other steroidal inhibitor, galeterone. All four non-steroidal inhibitors demonstrated less potency than abiraterone and galeterone. Of the non-steroidal inhibitors evaluated, (*S*)-orteronel was the most potent inhibitor of both pregnenolone and progesterone hydroxylase reactions, but was still 6- or 13-fold less potent than abiraterone, respectively. The other non-steroidal inhibitor, (*S*)-seviteronel, was an equipotent inhibitor of the pregnenolone hydroxylation

compared to (S)-orteronel and the second most potent non-steroidal inhibitor of the progesterone hydroxylase reaction. (R)-Orteronel demonstrated significantly lower affinity than its S enantiomer for inhibition of both hydroxylation reactions. Consistent with poor inhibition of the 17,20-lyase reaction and low binding affinity, (R)-seviteronel exhibited the lowest potency for inhibition of progesterone hydroxylation and thus was not evaluated further.

Comparison of IC_{50} values for 17,20-lyase inhibition and progesterone or pregnenolone hydroxylation can be used to evaluate inhibitor selectivity for the targeted reaction (17,20-lyase) over the non-targeted reactions (progesterone and pregnenolone hydroxylase) (Table 3, representative data shown in Figure 8). The most selective inhibitors exhibit high IC_{50} values for the off-target hydroxylase reaction and low IC_{50} values for the targeted 17,20-lyase reaction. Selectivity is defined herein as the ratio of 17-hydroxylase IC_{50}/17,20-lyase IC_{50}. A selectivity factor of 1 therefore indicates no selectivity for 17,20-lyase reaction, while higher selectivity factors indicate more selectivity toward desired inhibition of the 17,20 lyase reaction. All inhibitors evaluated were more effective in suppressing the 17,20-lyase reaction than either 17-hydroxylase reaction, and therefore all have selectivity factors greater than 1. The steroidal inhibitors abiraterone and galeterone demonstrated between 1.3 and 3.3-fold selectivity for 17,20-lyase inhibition over hydroxylase inhibition. The S enantiomer of non-steroidal orteronel showed little selectivity against pregnenolone hydroxylation (3.3-fold) and only slightly higher selectivity (4.5-fold) against progesterone hydroxylation (Figure 8A). Its enantiomer, (R)-orteronel, exhibited greater selectivity for inhibition of the targeted 17,20-lyase reaction over both progesterone hydroxylation (Figure 8B) and pregnenolone hydroxylation (8-fold and 11-fold, respectively). In contrast, the non-steroidal inhibitor (S)-seviteronel did not demonstrate significant selectivity for 17,20-lyase inhibition compared to the steroidal inhibitors (2.7- and

18

DMD # 75317

2.1- fold selectivity against progesterone and pregnenolone hydroxylation, respectively). Similarly, (*R*)-seviteronel demonstrated only 2.3-fold selectivity for 17,20-lyase inhibition against progesterone hydroxylase inhibition. Due to its poor potency and lack of observed selectivity against progesterone hydroxylation, (*R*)-seviteronel was not evaluated for inhibition of pregnenolone hydroxylation.

DISCUSSION

Cytochrome P450 17A1 inhibitors that have undergone clinical trials have all been individually functionally evaluated in one context or another. These *in vitro* studies typically determined IC_{50} values, which can vary depending on substrate concentration and other experimental conditions. This is demonstrated by the wide range of reported values for abiraterone (Table 1), making it exceedingly difficult to compare between studies. Such comparisons are becoming more essential with development of second-generation steroidal and non-steroidal inhibitors targeting selective inhibition of the 17,20-lyase reaction over 17α-hydroxylation. The current study uses tightly-defined conditions to determine IC_{50} values across inhibitors. Such comparisons establish rank order potency and determine whether selective inhibition of the 17,20-lyase reaction is indeed possible for compounds that likely coordinate the heme.

Steroidal abiraterone and galeterone were the most potent for the desired inhibition of the 17,20-lyase reaction. This is consistent with binding data demonstrating very high affinity of these compounds for the CYP17A1 active site (DeVore and Scott, 2012). Abiraterone exhibited the highest potency overall ($IC_{50}=36 \pm 3$ nM), broadly consistent with previous studies in microsomes and purified protein systems (3 and 27 nM (Potter et al., 1995; Yamaoka et al.,

19

2012; Rafferty et al., 2014)). Galeterone exhibited ~3-fold lower potency. Since abiraterone and galeterone are both based on the steroidal scaffold, these differences suggest the galeterone's benzimidazole coordinates the heme iron less effectively than abiraterone's pyridine. A previous report of galeterone as a more potent inhibitor than abiraterone in a whole cell system may reflect other factors including differences in cellular penetration (Handratta et al., 2005).

The most potent non-steroidal inhibitor was (*S*)-orteronel (IC$_{50}$ = 210 ± 20), which was 5.8-fold less potent than abiraterone for inhibiting the 17,20-lyase reaction. (*S*)-Seviteronel exhibited lower potency (IC$_{50}$ = 430 ± 40 nM; 12-fold lower than abiraterone). The R enantiomers of both non-steroidal inhibitors demonstrated even lower potency for 17,20-lyase inhibition. (*R*)-Orteronel was 2.2-fold less potent than (*S*)-orteronel, while (*R*)-seviteronel was ~12-fold less potent than its *S* enantiomer. (*R*)-seviteronel also binds the CYP17A1 iron with a much lower affinity than (*S*)-seviteronel. Overall, these results suggest S stereochemistry is advantageous for potent 17,20-lyase inhibition in these non-steroidal agents.

Rank order potency determined by the current study is broadly consistent with the clinical success of CYP17A1 inhibitors pursued to date. Abiraterone was highly successful in clinical trials, improving overall survival in Phase III clinical trials (Fizazi et al., 2012). Decreased potency for 17,20-lyase inhibition by (*S*)-orteronel when compared to abiraterone is consistent with its failure to achieve a similar end point (Saad et al., 2015). Based on these results, it is improbable that an even less potent inhibitor of 17,20-lyase activity such as (*S*)-seviteronel would demonstrate improved efficacy in a clinical setting--if overall survival is solely modulated by CYP17A1 inhibition. However, this is almost certainly not the case, as steroidal inhibitors have been reported to both antagonize (Handratta et al., 2005; Richards et al., 2012) and cause degradation of the androgen receptor (Yu et al., 2014), and (*S*)-seviteronel has also

been reported to act as an anti-androgen (Toren et al., 2014). Nonetheless, inhibition of 17,20-lyase activity of CYP17A1 is a primary contributor to success of these compounds in a clinical setting.

CYP17A1 inhibitors can also block 17α-hydroxylation necessary for glucocorticoid biosynthesis, resulting in side effects including hypertension and peripheral edema (Attard et al., 2012; Fizazi et al., 2012). Abiraterone selectivity for the 17,20-lyase reaction over the 17α-hydroxylation reportedly ranges from 0.1-fold to 1.4-fold depending on the conditions used (Potter et al., 1995; Yamaoka et al., 2012; Rafferty et al., 2014). Using purified CYP17A1 and partner proteins, we observed 2- and 3.3-fold selectivity for 17,20-lyase inhibition over progesterone and pregnenolone 17α-hydroxylation, respectively. Galeterone demonstrated ~1.5-fold selectivity for 17,20-lyase inhibition over inhibition of either hydroxylation reaction, suggesting it may cause similar side effects.

Non-steroidal inhibitors (*S*)-orteronel and (*S*)-seviteronel are reported to be 5- and 10-fold more selective for 17,20-lyase inhibition compared to 17α-hydroxylase inhibition (Yamaoka et al., 2012; Rafferty et al., 2014). Thus, they have been developed as CYP17A1 inhibitors with potentially improved side effect profiles. In the current study, (*S*)-orteronel demonstrated 3.3- to 4.5-fold selectivity for 17,20-lyase inhibition. It is unknown if this slight increase in selectivity compared to abiraterone would significantly improve the side effects, as (*S*)-orteronel was still co-administered with prednisone in clinical trials (Saad et al., 2015).

In the current study, (*S*)-seviteronel demonstrated only 2- and 3-fold lyase selectivity, contrasting with the 10-fold selectivity for lyase inhibition over pregnenolone 17α-hydroxylase inhibition previously reported in yeast microsome studies (Rafferty et al., 2014). There are several possible explanations for this apparent discrepancy. In earlier work the ratios of

21

CYP17A1 to cofactors NADPH-cytochrome P450 reductase and cytochrome b_5 were either not known or not reported, and may have an effect on the enzymatic turnover, the K_m, and IC$_{50}$ values. Additionally, the hydroxylase substrate concentrations may have differed from the K_m. Substrate concentrations $>K_m$ introduce bias against competitive inhibitors and could result in artificially high hydroxylase IC$_{50}$ values. Clinical trials for (S)-seviteronel are still recruiting, but similar selectivity to abiraterone suggests that this non-steroidal inhibitor may produce similar side effects.

Both non-steroidal inhibitors in clinical trials include stereocenters with an S configuration. These enantiomers were pursued in the clinical trials because they were more potent 17,20-lyase inhibitors than their R enantiomers (Kaku et al., 2011; Rafferty et al., 2014). There have been no previous reports on the selectivity of inhibition by the R enantiomers. In the current study, (R)-seviteronel demonstrated significantly lower potency than (S)-seviteronel, with no significant difference in selectivity for the 17,20-lyase reaction compared to progesterone hydroxylation. Although (R)-orteronel is much less potent for lyase inhibition, it exhibited better selectivity. (R)-Orteronel inhibited the 17,20-lyase reaction 8-fold better than progesterone hydroxylation and 11-fold better than pregnenolone hydroxylation. This indicates that the configuration of orteronel's stereocenter can have an impact on selectivity for 17,20-lyase inhibition.

Although (R)-orteronel's decreased potency in suppressing 17,20-lyase activity would make it a poor candidate for clinical development, it could provide insights into possible mechanisms for selective 17,20-lyase inhibition. The 2.2 Å crystal structure of CYP17A1 co-crystallized with a racemic mixture of (S)- and (R)- orteronel revealed that (R)-orteronel binds exclusively to one of the two conformations typically observed for CYP17A1. In this CYP17A1

conformation (molecule A/B), (*R*)-orteronel is coordinated to the heme iron and also hydrogen

bonds with N202 of the F helix, like steroidal inhibitors (DeVore and Scott, 2012). The second

conformation of CYP17A1 (molecule C/D), differing especially in the region between helices F

and G, appears to selectively bind (*S*)-orteronel (Figure 7). (*S*)-Orteronel also coordinates the

heme iron but does not interact with F-helix residues, instead hydrogen bonding with R239 on

the G helix and D298 on the I helix. Only this latter CYP17A1 conformation has an F/G loop

that forms a peripheral ligand binding site. This region of membrane P450 enzymes is highly

flexible and embedded in the endoplasmic reticulum membrane. Although both F/G

conformations are observed in all CYP17A1 structures with various steroidal inhibitors and

substrates determined to date, all of these ligands adopt the same orientation, regardless of

CYP17A1 conformations. However, a mix of (*R*)- and (*S*)-orteronel are not observed in the

CYP17A1 active site. Instead (*S*)-orteronel is selectively bound to the CYP17A1 F/G

conformation accommodating a peripheral ligand, while (*R*)-orteronel selectively binds the

active site of CYP17A1 displaying the alternate conformation of this loop that does not bind a

peripheral ligand.

Differing conformations of this F/G loop have generally been implicated in substrate

access to P450 active sites (Poulos and Johnson, 2005). In telost fish the processivity of the

CYP17A1 reactions is correlated with whether or not orteronel is selective for 17,20-lyase

inhibition over hydroxylase inhibition (Pallan et al., 2015a). For substrates more likely to leave

the active site after the initial hydroxylation and prior to the 17,20-lyase reaction, (*S*)-orteronel

demonstrated ~10-fold selectivity for 17,20-lyase inhibition. In contrast, for substrates less

likely to dissociate from the active site between 17-hydroxylase and 17,20-lyase reactions, only

23

2-fold selectivity for 17,20-lyase inhibition was observed. Similar processivity studies for human CYP17A1 with different substrates have not yet been reported.

Steroid binding in the F/G region has now been reported for several human cytochrome P450 enzymes. A structure of steroidogenic CYP21A2 revealed with a low-affinity, partially-occupied steroid in this region(Pallan et al., 2015b). CYP3A4, the major human drug metabolizing P450, binds progesterone in this region(Williams et al., 2004). The F/G region is typically a major component of the most hydrophobic surface of mammalian P450 enzymes. It is also thought to be buried in the membrane and the major entry point for generally hydrophobic substrates to access the active site. Thus, steroid binding in this region may be adventitious association driven by hydrophobic interactions or part of an initial substrate docking region before steroids advance into the buried active site. Although cooperativity is not apparent in (*S*)-orteronel binding to CYP17A1, ligand binding to P450 enzymes is detected by observing spectral changes associated with interactions near the heme and peripheral ligand binding would not necessarily be apparent. It is known that F/G residues play a role in the homotrophic cooperativity of progesterone metabolism in CYP3A4(Harlow and Halpert, 1998; Domanski et al., 2001), but the physiological significance of peripheral ligand binding should be further evaluated.

In conclusion, rank order potency and selectivity were established for *in vitro* inhibition of CYP17A1, with steroidal compounds more potent than the non-steroidal inhibitors seviteronel and orteronel. Ten-fold selectivity for 17,20-lyase inhibition previously reported for (*S*)-seviteronel was not observed, but less potent (*R*)-orteronel was more selective (8- to 11-fold). Structures with non-steroidal inhibitors reveal coordination of the heme iron, but demonstrate that different conformations of the F/G region can correlate with the binding of distinct orteronel

24

enantiomers in the active site and the capacity for peripheral binding of a ligand molecule. While iron coordination of inhibitors in the active site is consistent with competitive, non-selective inhibition, both conformational selection for binding of some inhibitors and the differential presence of a peripheral ligand raise the possibility of differentially modulating CYP17A1 function via features outside the active site. Improved understanding of CYP17A1 structure/function relationships could help inform the development of more selective inhibitors, thereby improving prostate cancer treatment.

AUTHORSHIP CONTRIBUTIONS

Participated in research design: Petrunak, Rogers, Aubé, Scott

Conducted experiments: Petrunak, Rogers, Scott

Contributed new reagents or analytical tools: none

Performed data analysis: Petrunak, Rogers, Aubé, Scott

Wrote or contributed to the writing of the manuscript: Petrunak, Rogers, Aubé, Scott

REFERENCES

Adams PD, Afonine PV, Bunkoczi G, Chen VB, Davis IW, Echols N, Headd JJ, Hung LW,
Kapral GJ, Grosse-Kunstleve RW, McCoy AJ, Moriarty NW, Oeffner R, Read RJ,
Richardson DC, Richardson JS, Terwilliger TC, and Zwart PH (2010) PHENIX: a
comprehensive Python-based system for macromolecular structure solution. *Acta
Crystallogr, Sect D: Biol Crystallogr* **66:**213-221.

Al-Masoudi NA, Ali DS, Saeed B, Hartmann RW, Engel M, Rashid S, and Saeed A (2014) New
CYP17 hydroxylase inhibitors: synthesis, biological evaluation, QSAR, and molecular
docking study of new pregnenolone analogs. *Arch Pharm (Weinheim, Ger)* **347:**896-907.

Arlt W, Martens JW, Song M, Wang JT, Auchus RJ, and Miller WL (2002) Molecular evolution
of adrenarche: structural and functional analysis of p450c17 from four primate species.
Endocrinology **143:**4665-4672.

Attard G, Reid AH, Auchus RJ, Hughes BA, Cassidy AM, Thompson E, Oommen NB, Folkerd
E, Dowsett M, Arlt W, and de Bono JS (2012) Clinical and biochemical consequences of
CYP17A1 inhibition with abiraterone given with and without exogenous glucocorticoids
in castrate men with advanced prostate cancer. *J Clin Endocrinol Metab* **97:**507-516.

Attard G, Reid AH, Yap TA, Raynaud F, Dowsett M, Settatree S, Barrett M, Parker C, Martins
V, Folkerd E, Clark J, Cooper CS, Kaye SB, Dearnaley D, Lee G, and de Bono JS (2008)
Phase I clinical trial of a selective inhibitor of CYP17, abiraterone acetate, confirms that
castration-resistant prostate cancer commonly remains hormone driven. *J Clin Oncol*
26:4563-4571.

Auchus RJ (2001) The genetics, pathophysiology, and management of human deficiencies of
P450c17. *Endocrinol Metab Clin North Am* **30:**101-119.

Auchus RJ, Lee TC, and Miller WL (1998) Cytochrome b_5 augments the 17,20-lyase activity of human P450c17 without direct electron transfer. *J Biol Chem* **273:**3158-3165.

Bruno RD, Vasaitis TS, Gediya LK, Purushottamachar P, Godbole AM, Ates-Alagoz Z, Brodie AM, and Njar VC (2011) Synthesis and biological evaluations of putative metabolically stable analogs of VN/124-1 (TOK-001): head to head anti-tumor efficacy evaluation of VN/124-1 (TOK-001) and abiraterone in LAPC-4 human prostate cancer xenograft model. *Steroids* **76:**1268-1279.

Copeland RA (2013) *Evaluation of enzyme inhibitors in drug discovery. A guide for medicinal chemists and pharmacologists*. John Wiley & Sons, Hoboken, NJ.

DeVore NM and Scott EE (2012) Structures of cytochrome P450 17A1 with prostate cancer drugs abiraterone and TOK-001. *Nature* **482:**116-119.

Domanski TL, He YA, Khan KK, Roussel F, Wang Q, and Halpert JR (2001) Phenylalanine and tryptophan scanning mutagenesis of CYP3A4 substrate recognition site residues and effect on substrate oxidation and cooperativity. *Biochemistry* **40:**10150-10160.

Edwards BK, Noone AM, Mariotto AB, Simard EP, Boscoe FP, Henley SJ, Jemal A, Cho H, Anderson RN, Kohler BA, Eheman CR, and Ward EM (2014) Annual report to the nation on the status of cancer, 1975-2010, featuring prevalence of comorbidity and impact on survival among persons with lung, colorectal, breast, or prostate cancer. *Cancer* **120:**1290-1314.

Emsley P, Lohkamp B, Scott WG, and Cowtan K (2010) Features and development of Coot. *Acta Crystallogr, Sect D: Biol Crystallogr* **66:**486-501.

Fizazi K, Scher HI, Molina A, Logothetis CJ, Chi KN, Jones RJ, Staffurth JN, North S, Vogelzang NJ, Saad F, Mainwaring P, Harland S, Goodman OB, Jr., Sternberg CN, Li

JH, Kheoh T, Haqq CM, de Bono JS, and Investigators C-A- (2012) Abiraterone acetate for treatment of metastatic castration-resistant prostate cancer: final overall survival analysis of the COU-AA-301 randomised, double-blind, placebo-controlled phase 3 study. *Lancet Oncol* **13:**983-992.

Geller J (1993) Basis for hormonal management of advanced prostate cancer. *Cancer* **71:**1039-1045.

Gilep AA, Sushko TA, and Usanov SA (2011) At the crossroads of steroid hormone biosynthesis: the role, substrate specificity and evolutionary development of CYP17. *Biochim Biophys Acta* **1814:**200-209.

Gomez L, Kovac JR, and Lamb DJ (2015) CYP17A1 inhibitors in castration-resistant prostate cancer. *Steroids* **95:**80-87.

Handratta VD, Vasaitis TS, Njar VC, Gediya LK, Kataria R, Chopra P, Newman D, Jr., Farquhar R, Guo Z, Qiu Y, and Brodie AM (2005) Novel C-17-heteroaryl steroidal CYP17 inhibitors/antiandrogens: synthesis, in vitro biological activity, pharmacokinetics, and antitumor activity in the LAPC4 human prostate cancer xenograft model. *J Med Chem* **48:**2972-2984.

Harlow GR and Halpert JR (1998) Analysis of human cytochrome P450 3A4 cooperativity: construction and characterization of a site-directed mutant that displays hyperbolic steroid hydroxylation kinetics. *Proc Natl Acad Sci U S A* **95:**6636-6641.

Jagusch C, Negri M, Hille UE, Hu Q, Bartels M, Jahn-Hoffmann K, Pinto-Bazurco Mendieta MA, Rodenwaldt B, Muller-Vieira U, Schmidt D, Lauterbach T, Recanatini M, Cavalli A, and Hartmann RW (2008) Synthesis, biological evaluation and molecular modelling studies of methyleneimidazole substituted biaryls as inhibitors of human 17alpha-

hydroxylase-17,20-lyase (CYP17). Part I: Heterocyclic modifications of the core structure. *Bioorg Med Chem* **16:**1992-2010.

Jefcoate CR (1978) Measurement of substrate and inhibitor binding to microsomal cytochrome P-450 by optical-difference spectroscopy. *Methods Enzymol* **52:**258-279.

Kabsch W (2010) XDS. *Acta Crystallogr, Sect D: Biol Crystallogr* **66:**125-132.

Kaku T, Hitaka T, Ojida A, Matsunaga N, Adachi M, Tanaka T, Hara T, Yamaoka M, Kusaka M, Okuda T, Asahi S, Furuya S, and Tasaka A (2011) Discovery of orteronel (TAK-700), a naphthylmethylimidazole derivative, as a highly selective 17,20-lyase inhibitor with potential utility in the treatment of prostate cancer. *Bioorg Med Chem* **19:**6383-6399.

Katagiri M, Kagawa N, and Waterman MR (1995) The role of cytochrome b_5 in the biosynthesis of androgens by human P450c17. *Arch Biochem Biophys* **317:**343-347.

McCoy AJ, Grosse-Kunstleve RW, Adams PD, Winn MD, Storoni LC, and Read RJ (2007) Phaser crystallographic software. *J Appl Crystallogr* **40:**658-674.

Montgomery RB, Mostaghel EA, Vessella R, Hess DL, Kalhorn TF, Higano CS, True LD, and Nelson PS (2008) Maintenance of intratumoral androgens in metastatic prostate cancer: a mechanism for castration-resistant tumor growth. *Cancer Res* **68:**4447-4454.

O'Donnell A, Judson I, Dowsett M, Raynaud F, Dearnaley D, Mason M, Harland S, Robbins A, Halbert G, Nutley B, and Jarman M (2004) Hormonal impact of the 17alpha-hydroxylase/C(17,20)-lyase inhibitor abiraterone acetate (CB7630) in patients with prostate cancer. *Br J Cancer* **90:**2317-2325.

Pallan PS, Nagy LD, Lei L, Gonzalez E, Kramlinger VM, Azumaya CM, Wawrzak Z, Waterman MR, Guengerich FP, and Egli M (2015a) Structural and kinetic basis of steroid

17alpha,20-lyase activity in teleost fish cytochrome P450 17A1 and its absence in cytochrome P450 17A2. *J Biol Chem* **290:**3248-3268.

Pallan PS, Wang C, Lei L, Yoshimoto FK, Auchus RJ, Waterman MR, Guengerich FP, and Egli M (2015b) Human cytochrome P450 21A2, the major steroid 21-hydroxylase: structure of the enzyme/progesterone substrate comples and rate-limiting C-H bond cleavage. *J Biol Chem* **290:**13128-13143.

Petrunak EM, DeVore NM, Porubsky PR, and Scott EE (2014) Structures of human steroidogenic cytochrome P450 17A1 with substrates. *J Biol Chem* **289:**32952-32964.

Potter GA, Barrie SE, Jarman M, and Rowlands MG (1995) Novel steroidal inhibitors of human cytochrome P45017 alpha (17 alpha-hydroxylase-C17,20-lyase): potential agents for the treatment of prostatic cancer. *J Med Chem* **38:**2463-2471.

Poulos TL and Johnson EF (2005) Structures of Cytochrome P450 Enzymes, in: *Cytochrome P450: Structure, Mechanism, and Biochemistry* (Ortiz de Montellano P ed), Kluwer Academic / Plenum Publishers, New York.

Rafferty SW, Eisner JR, Moore WR, Schotzinger RJ, and Hoekstra WJ (2014) Highly-selective 4-(1,2,3-triazole)-based P450c17a 17,20-lyase inhibitors. *Bioorg Med Chem Lett* **24:**2444-2447.

Richards J, Lim AC, Hay CW, Taylor AE, Wingate A, Nowakowska K, Pezaro C, Carreira S, Goodall J, Arlt W, McEwan IJ, de Bono JS, and Attard G (2012) Interactions of abiraterone, eplerenone, and prednisolone with wild-type and mutant androgen receptor: a rationale for increasing abiraterone exposure or combining with MDV3100. *Cancer Res* **72:**2176-2182.

Ryan CJ, Smith MR, Fong L, Rosenberg JE, Kantoff P, Raynaud F, Martins V, Lee G, Kheoh T, Kim J, Molina A, and Small EJ (2010) Phase I clinical trial of the CYP17 inhibitor abiraterone acetate demonstrating clinical activity in patients with castration-resistant prostate cancer who received prior ketoconazole therapy. *J Clin Oncol* **28:**1481-1488.

Saad F, Fizazi K, Jinga V, Efstathiou E, Fong PC, Hart LL, Jones R, McDermott R, Wirth M, Suzuki K, MacLean DB, Wang L, Akaza H, Nelson J, Scher HI, Dreicer R, Webb IJ, de Wit R, and investigators E-P (2015) Orteronel plus prednisone in patients with chemotherapy-naive metastatic castration-resistant prostate cancer (ELM-PC 4): a double-blind, multicentre, phase 3, randomised, placebo-controlled trial. *Lancet Oncol* **16:**338-348.

Sandee D and Miller WL (2011) High-yield expression of a catalytically active membrane-bound protein: human P450 oxidoreductase. *Endocrinology* **152:**2904-2908.

Schrodinger, LLC (2010) The AxPyMOL Molecular Graphics Plugin for Microsoft PowerPoint, Version 1.0.

Toren P, Pham S, Kim S, Adomat H, Zoubeidi A, Moore WR, and Gleave ME (2014) Anticancer activity of the selective CYP17A1 inhibitor, VT-464, in preclinical models of castrate-resistant prostate cancer., in: *Genitourinary Cancers Symposium*, American Society of Clinical Oncology, Vancouver, BC, Canada.

Williams PA, Cosme J, Vinkovic DM, Ward A, Angove HC, Day PJ, Vonrhein C, Tickle IJ, and Jhoti H (2004) Crystal structures of human cytochrome P450 3A4 bound to metyrapone and progesterone. *Science* **305:**683-686.

Yamaoka M, Hara T, Hitaka T, Kaku T, Takeuchi T, Takahashi J, Asahi S, Miki H, Tasaka A, and Kusaka M (2012) Orteronel (TAK-700), a novel non-steroidal 17,20-lyase inhibitor:

effects on steroid synthesis in human and monkey adrenal cells and serum steroid levels

in cynomolgus monkeys. *J Steroid Biochem Mol Biol* **129:**115-128.

Yin L and Hu Q (2014) CYP17 inhibitors--abiraterone, C17,20-lyase inhibitors and multi-

targeting agents. *Nat Rev Urol* **11:**32-42.

Yu Z, Cai C, Gao S, Simon NI, Shen HC, and Balk SP (2014) Galeterone prevents androgen

receptor binding to chromatin and enhances degradation of mutant androgen receptor.

Clin Cancer Res **20:**4075-4085.

Zhao B, Lei L, Kagawa N, Sundaramoorthy M, Banerjee S, Nagy LD, Guengerich FP, and

Waterman MR (2012) Three-dimensional structure of steroid 21-hydroxylase

(cytochrome P450 21A2) with two substrates reveals locations of disease-associated

variants. *J Biol Chem* **287:**10613-10622.

DMD # 75317

FOOTNOTES

Funding sources

Reprint requests

Emily E. Scott, Department of Medicinal Chemistry, University of Michigan, 428 Church St., Ann Arbor, MI 48109

Numbered footnotes

EMP present address: Life Science Institute, University of Michigan, 210 Washtenaw Ave., Ann Arbor, MI 48109, petrunak@umich.edu

SAR present address: 2300 Trammell Crow Center, 2001 Ross Avenue, Dallas, TX, 75201

JA Present address: UNC Eshelman School of Pharmacy, 125 Mason Farm Road, CB 7363, University of North Carolina, Chapel Hill, Chapel Hill, NC 27599.

34

EES Present address: Department of Medicinal Chemistry, University of Michigan, 428 Church St., Ann Arbor, MI 48109

PDB ID Codes: The PDB ID codes for CYP17A1 bound to racemic orteronel and (S)-seviteronel are 5IRQ and 5IRV, respectively. Authors will release the atomic coordinates and experimental data upon article publication.

DMD # 75317

FIGURE LEGENDS

Figure 1. A) CYP17A1 mediates two major types of reactions, initial 17α-hydroxylation (blue) of pregnenolone or progesterone, followed by a 17,20-lyase reaction (magenta) on 17α-hydroxypregnenolone.   While only the latter 17,20-lyase reaction is necessary for androgen biosynthesis, downstream products of the hydroxylase reaction include important glucocorticoids such as cortisol.   Inhibition of CYP17A1 by abiraterone (green) inhibits both CYP17A1-mediated reaction types, resulting in the desired net decrease in androgens but an undesirable decrease in glucocorticoids.   The decrease in glucocorticoids results in an overproduction of mineralocorticoids as a result of adrenocorticotropin hormone feedback.   B) Abiraterone (green sticks) inhibits both CYP17A1 reactions by directly coordinating the CYP17A1 heme (black sticks with red iron sphere at center) required for catalysis.

Figure 2.   Difference spectra illustrate absorbance shifts associated with heteroatom coordination to the heme iron as (*S*)-orteronel is titrated into 100 nM CYP17A1 (shown). Similar shifts were observed for the other four non-steroidal inhibitors evaluated (not shown). Spectra with increasing inhibitor concentrations are shown from low to high concentrations (red to blue/violet).   The difference in absorbance between the resulting peak and trough (ΔAbsorbance) were used to evaluate the ligand binding affinity to CYP17A1.

Figure 3. A) Binding of non-steroidal inhibitor (*S*)-seviteronel to 100 nM CYP17A1 deviates from the tight-binding equation, consistent with very high affinity for the enzyme. The fit shown has an estimated K_d of 31 ± 7, which is likely the upper limit of the dissociation constant for this complex. B) In contrast, titration of 100 nM CYP17A1 with (*R*)-seviteronel reveals much lower affinity (K_d= 290 ± 10 nM) and has a much better fit to the tight-binding equation.

36

Figure 4. The contrasting ligand density in molecules C/D (panel A) compared to molecules A/B (panel B) in the 2.2 Å structure of CYP17A1 with orteronel supports binding of different enantiomers of orteronel in different molecules of the structure ((S)-orteronel in panel A, (R)-orteronel in panel B). Simulated annealing $2F_o$-F_c composite omit maps (contoured to 1.0 σ) are shown as blue mesh. (R)-orteronel, modeled into molecules A/B of the structure (panel B), does not fully satisfy electron density as indicated by the simulated annealing composite omit Fo-Fc map for molecule A (negative density shown in red mesh and positive density shown in green mesh, contoured to 3.0 σ), which may indicate a small amount of disorder. The same Fo-Fc map for (S)-orteronel indicates an excellent match between the density and the ligand model and so is not shown for clarity.

Figure 5. Interaction of A) (S)-orteronel and B) (R)-orteronel with CYP17A1 active site residues. All distances shown are averages for molecules A and B (in panel A) or C and D (in panel B).

Figure 6. The 3.1 Å structure of CYP17A1 with (S)-seviteronel. A) (S)-seviteronel (orange sticks) binds in the CYP17A1 active site coordinated to the heme (black sticks) iron (red sphere). Electron density for ligand and heme (blue mesh) is a simulated annealing 2Fo-Fc composite omit map contoured to 1.00 σ. B) Interactions between CYP17A1 active site and (S)-seviteronel. Distances shown are averages from all four molecules.
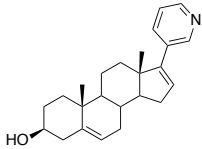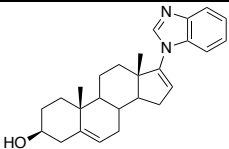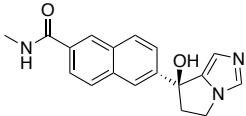
Figure 7. (R)-orteronel (magenta) and (S)-orteronel (teal) bind selectively to two distinct conformations of CYP17A1. A major structural difference between the two formations is the structure of the F/G loop, a region implicated in ligand entry and exit for other mammalian cytochrome P450 enzymes. An unknown ligand (Fo-Fc map in green mesh at 3.0 σ) is present only in the conformation that binds (S)-orteronel (teal).
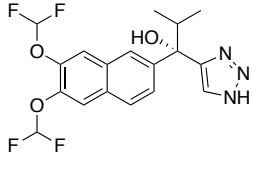
37

DMD # 75317

Figure 8. Differences in 17,20-lyase inhibition (solid lines) and progesterone hydroxylase inhibition (dashed lines) demonstrate less selectivity for 17,20-lyase inhibition by A) (*S*)-orteronel compared to B) (*R*)-orteronel.

38

TABLES

Table 1. Reported IC_{50} values for inhibitors of CYP17A1 that have undergone clinical trials

Inhibitor	FDA Approval Status	Reported 17,20-Lyase IC_{50} (nM)	Reported 17α-Hydroxylase IC_{50} (nM)	Reported 17,20-Lyase Selectivity[a]
Abiraterone	Approved	2.9-800 (Potter et al., 1995; Handratta et al., 2005; Yamaoka et al., 2012; Rafferty et al., 2014)	1.5-72 (Potter et al., 1995; Jagusch et al., 2008; Yamaoka et al., 2012; Al-Masoudi et al., 2014; Rafferty et al., 2014)	0.1- to 1.4-fold (Potter et al., 1995; Yamaoka et al., 2012; Rafferty et al., 2014)
Galeterone (TOK-001 or VN/124-1)	Phase III Clinical Trials	47-300 (Handratta et al., 2005; Bruno et al., 2011)	N/R[b]	N/R[b]
(S)-Orteronel (TAK-700)	Discontinued after Phase III Clinical Trials	19-140 (Kaku et al., 2011; Yamaoka et al., 2012)	760 (Yamaoka et al., 2012)	5-fold (Yamaoka et al., 2012)

	Phase II Clinical Trials	69 (Rafferty et al., 2014)	690 (Rafferty et al., 2014)	10-fold (Rafferty et al., 2014)
(S)-seviteronel (VT-464)				

[a]Versus progesterone or pregnenolone hydroxylation

[b]N/R: not reported

Table 2. Crystallographic data collection and refinement statistics for CYP17A1 with

nonsteroidal inhibitors orteronel and (*S*)-seviteronel.

	CYP17A1/racemic orteronel	CYP17A1/(*S*)-seviteronel
Data Collection		
Beamline	SSRL 7-1	SSRL 12-2
Space Group	$P2_12_12_1$	$P2_12_12_1$
Cell Dimensions (Å)	90.17, 153.20, 168.12	90.95, 153.50, 169.04
Molecules/a.u.	4	4
Resolution (Å)[a]	39.28-2.20 (2.32-2.20)	39.44-3.10 (3.27-3.10)
Total reflections[a]	871,993 (125,334)	142,288 (20,014)
Unique reflections[a]	118,993 (16,928)	43,069 (6,096)
Redundancy[a]	7.4 (7.4)	3.3 (3.3)
R_{pim}[a]	0.053 (0.608)	0.087 (0.579)
$<I/\sigma(I)>$[a]	14.0 (1.6)	8.4 (1.6)
Completeness (%)[a]	99.8 (99.0)	98.5 (96.5)
Refinement		
Resolution (Å)	39.29-2.20	39.44-3.10
No. reflections	117,964	42,930
R/R_{free} (%)	20.13/24.86	19.51/24.80
Ramachandran (%)		
Favored	96.07	94.67
Allowed	3.93	5.07
Outliers	0.00	0.27
No. atoms/B factors (Å^2)		
Protein	14,901/47.4	15,025/62.5
Ligand	92/44.5	112/44.5
Heme	172/33.7	172/48.7
Water	525/41.9	0
RMSD bond (Å)	0.005	0.004
RMSD angle (°)	0.618	0.810
Coordinate error (max. likelihood based) (Å)	0.28	0.44

[a]Statistics for highest resolution shell are shown in parentheses.
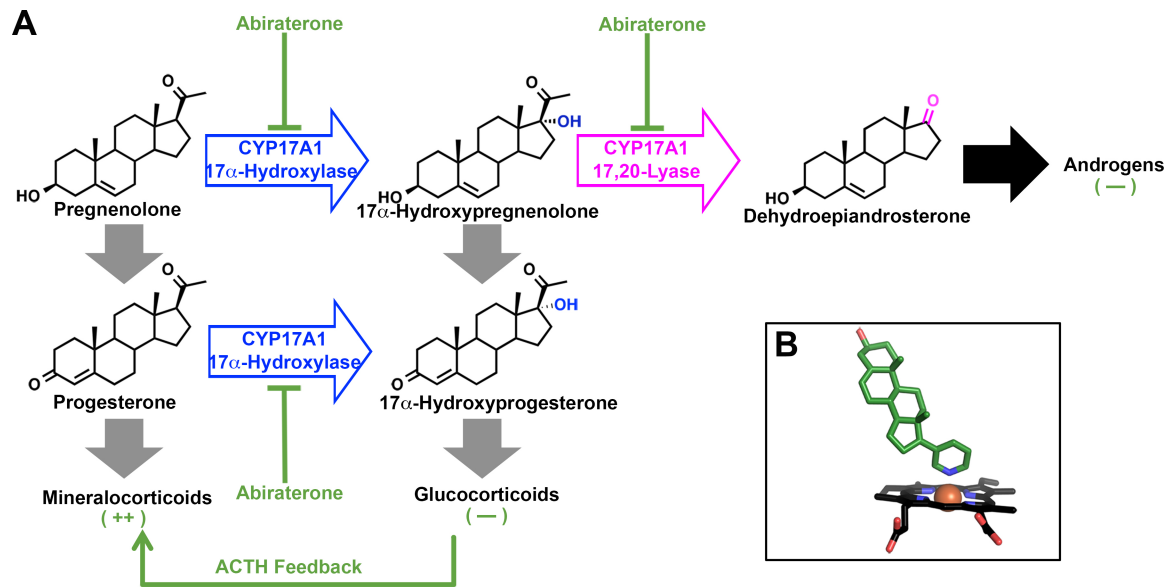
DMD # 75317

Table 3. Summary of IC_{50} values for 17α-hydroxypregnenolone 17,20-lyase inhibition (targeted reaction), progesterone and pregnenolone hydroxylation (off-target reactions), and resulting selectivity ratios. IC_{50} values are the average of two independent experiments ± standard error. Within each experiment, each inhibitor concentration was evaluated in duplicate or triplicate.

Inhibitor	Lyase IC_{50} (nM)	Progesterone Hydroxylase IC_{50} (nM)	Progesterone Hydroxylase $\dfrac{IC_{50}}{\text{Lyase } IC_{50}}$	Pregnenolone Hydroxylase IC_{50} (nM)	Pregnenolone Hydroxylase $\dfrac{IC_{50}}{\text{Lyase } IC_{50}}$
Abiraterone	36 ± 2	76 ± 5	2.1 ± 0.2	121 ± 7	3.3 ± 0.3
Galeterone	100 ± 10	130 ± 10	1.3 ± 0.2	150 ± 20	1.5 ± 0.3
(S)-orteronel	210 ± 20	950 ± 70	4.5 ± 0.5	700 ± 100	3.3 ± 0.6
(R)-orteronel	460 ± 90	4000 ± 300	8 ± 2	5000 ± 1000	11 ± 3
(S)-seviteronel	430 ± 40	1170 ± 90	2.7 ± 0.3	700 ± 100	2.1 ± 0.4
(R)-seviteronel	5000 ± 1000	11300 ± 900	2.3 ± 0.5	N/D[a]	N/D[a]

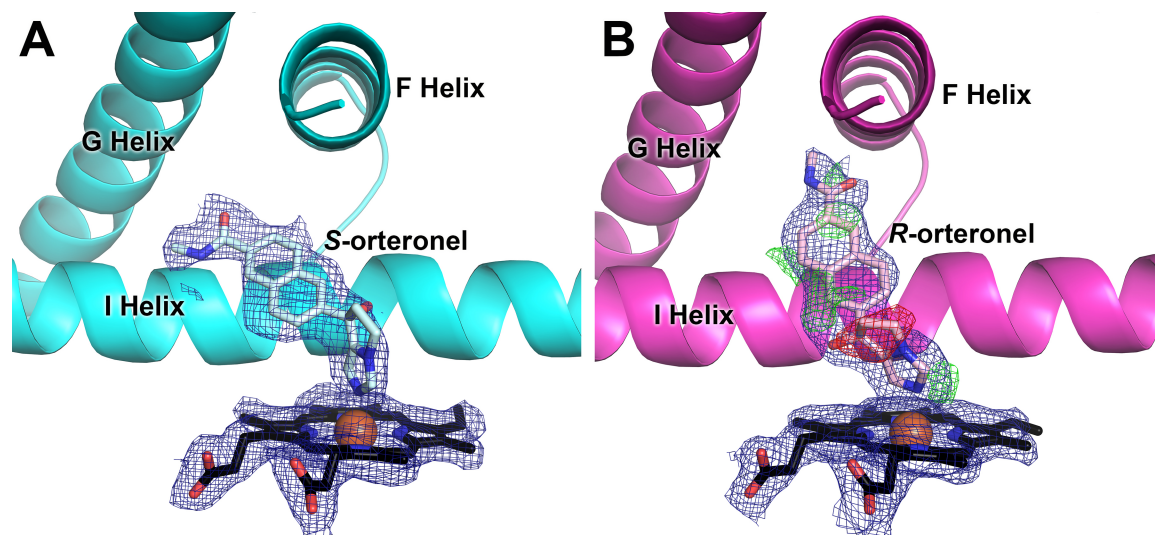[a]ND: Not Determined

42
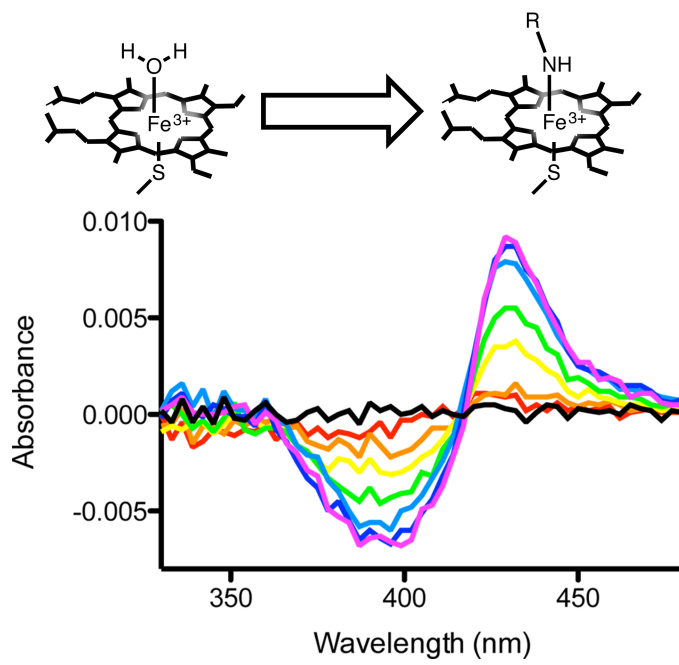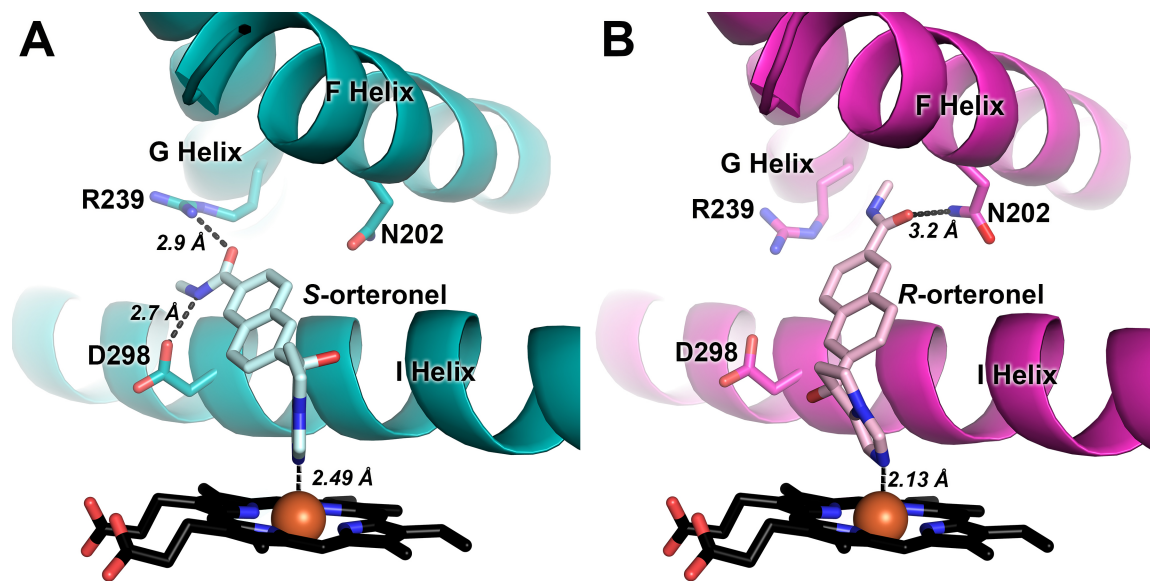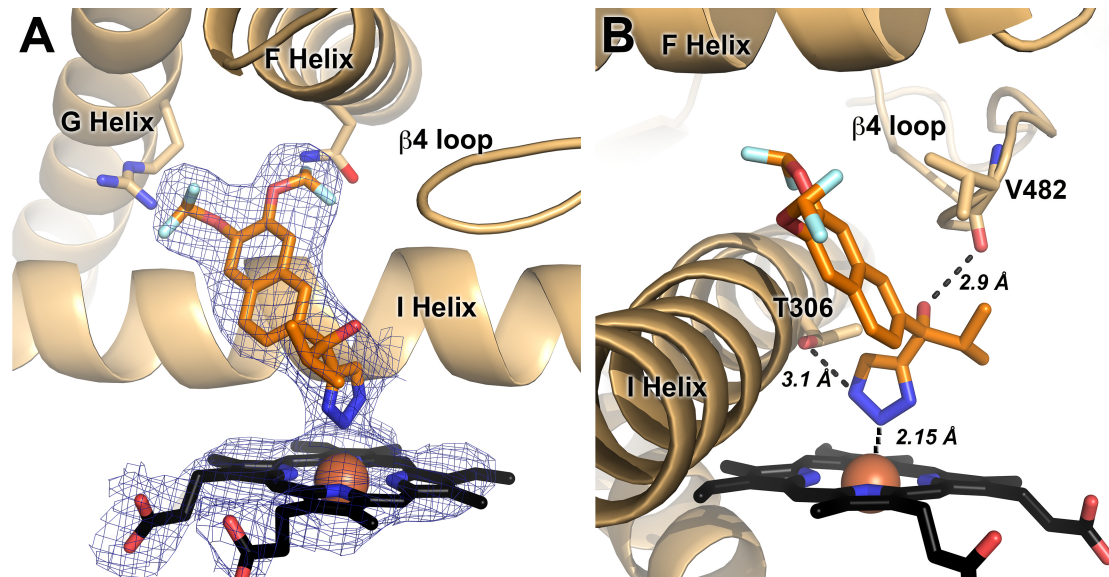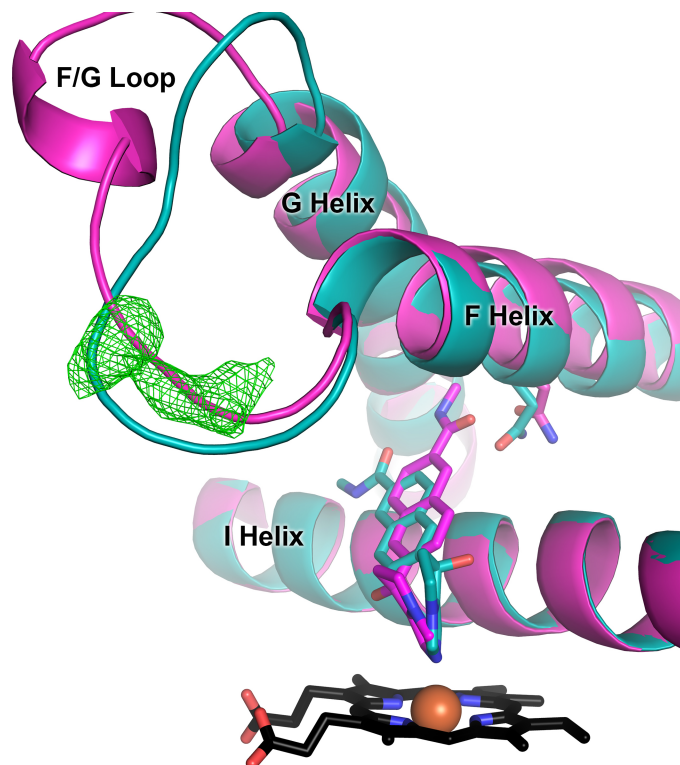
FIGURES

Figure 1
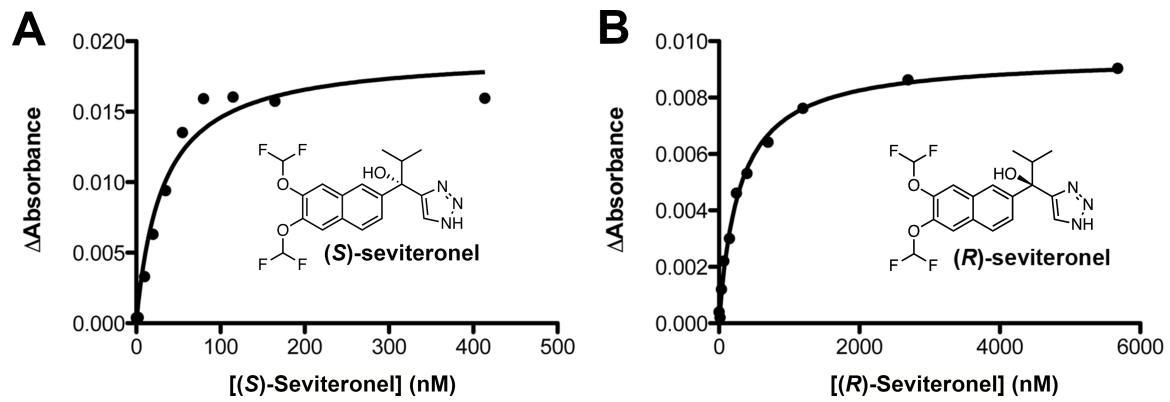
Figure 2

Figure 3.

Figure 4.

DMD # 75317

Figure 5.

Figure 6.

Figure 7.

DMD # 75317

Figure 8.